REPORT DOCUMENTATION PAGE

Form Approved
OMB No. 0704-0188

1. REPORT DATE *(DD-MM-YYYY)*	**2. REPORT TYPE**	**3. DATES COVERED** *(From – To)*
01-12-2016	Interim	Jan 1 2014-31 Dec 2016

4. TITLE AND SUBTITLE
Investigation of superparamagnetic (Fe3O4) nanoparticles and magnetic field exposures on CHO-K1 cell line

5a. CONTRACT NUMBER
In-house

5b. GRANT NUMBER

5c. PROGRAM ELEMENT NUMBER
62202F

6. AUTHOR(S)
Zachary Coker[1,4], Larry Estlack[2], Saber M. Hussain[3], Tae-Youl Choi[4], Bennett L. Ibey[1]

5d. PROJECT NUMBER
7757

5e. TASK NUMBER
B3

5f. WORK UNIT NUMBER
60/H0AW

7. PERFORMING ORGANIZATION NAME(S) AND ADDRESS(ES)
1Radio Frequency Bioeffects Branch, Bioeffects Division, Human Effectiveness Directorate, 711th Human Performance Wing, Air Force Research Laboratory, JBSA Fort Sam Houston, TX
2General Dynamics Information Technology, JBSA Fort Sam Houston, TX
3Bioeffects Division, Human Effectiveness Directorate, 711th Human Performance Wing, Air Force Research Laboratory, WPAFB, Dayton, OH
4Department of Mechanical and Energy Engineering, University of North Texas, Denton, TX

8. PERFORMING ORGANIZATION REPORT NUMBER
N/A

9. SPONSORING / MONITORING AGENCY NAME(S) AND ADDRESS(ES)
Air Force Material Command, Air Force Research Laboratory, 711th Human Performance Wing, Human Effectiveness Directorate, Bioeffects Division, Radio Frequency Bioeffects Branch, (711 HPW/RHDR) , 4141 Petroleum Drive, JBSA Fort Sam Houston, Texas 78234-2644

10. SPONSOR/MONITOR'S ACRONYM(S)
711 HPW/RHD_
TSRL-2016-0236

11. SPONSOR/MONITOR'S REPORT NUMBER(S)
AFRL-RH-FS-PC-2016-XXXX

12. DISTRIBUTION / AVAILABILITY STATEMENT
Distribution A. Approved for Public Release, TSRL-2016-0236

13. SUPPLEMENTARY NOTES

14. ABSTRACT

Rapid development in nanomaterial synthesis and surface functionalization has led to advanced studies in actuation and manipulation of cellular functions for biomedical applications. One common actuation technique employs externally applied magnetic fields to manipulate magnetic nanomaterials within cells in order to drive or trigger desired effects. While cellular interactions with low-frequency magnetic fields and nanoparticles have been extensively studied, the fundamental mechanisms behind these interactions remain poorly understood. Additionally, modern investigations on these concurrent exposure conditions have been limited in scope, and difficult to reproduce. This study presents an easily reproducible method of investigating the biological impact of concurrent magnetic field and nanoparticle exposure conditions using a well-defined in-vitro CHO-K1 cell line model, with the purpose of establishing grounds for in-depth fundamental studies of the mechanisms driving cellular-level interactions. Cells were cultured under various nanoparticle and magnetic field exposure conditions singly or in combination from 0 to 500 μg/ml nanoparticle concentrations and DC, 50 Hz, or 100 Hz magnetic fields with 2.0 mT flux density. Cells were then observed by confocal fluorescence microscopy, and subject to biological assays to determine the effects of concurrent extreme-low frequency magnetic field and nanoparticle exposures on cell-nanoparticle interactions, such as particle uptake and cell viability by MTT assay. Current results indicate little to no variation in effect on cell cultures based on magnetic field parameters alone; however, it is clear that deleterious synergistic effects of concurrent exposure conditions exist based on a significant decrease in cell viability when exposed to high concentrations of nanoparticles and concurrent magnetic field

15. SUBJECT TERMS

16. SECURITY CLASSIFICATION OF:			**17. LIMITATION OF ABSTRACT**	**18. NUMBER OF PAGES**	**19a. NAME OF RESPONSIBLE PERSON**
a. REPORT	**b. ABSTRACT**	**c. THIS PAGE**			**19b. TELEPHONE NUMBER** (include area code)
Unclassified	Unclassified	Unclassified	SAR	6	N/A

Investigation of superparamagnetic (Fe3O4) nanoparticles and magnetic field exposures on CHO-K1 cell line

Zachary Coker, Larry Estlack, Saber Hussain, Tae-Youl Choi, Bennett L. Ibey

Zachary Coker, Larry Estlack, Saber Hussain, Tae-Youl Choi, Bennett L. Ibey, "Investigation of superparamagnetic (Fe3O4) nanoparticles and magnetic field exposures on CHO-K1 cell line," Proc. SPIE 9706, Optical Interactions with Tissue and Cells XXVII, 97061Y (7 March 2016); doi: 10.1117/12.2220816

SPIE.

Event: SPIE BiOS, 2016, San Francisco, California, United States

Investigation of superparamagnetic (Fe_3O_4) nanoparticles and magnetic field exposures on CHO-K1 cell line

Zachary Coker[14], Larry Estlack[2], Saber Hussain[3], Tae-Youl Choi[4], Bennett L. Ibey[1]
[1]Radio Frequency Bioeffects Branch, Bioeffects Division, Human Effectiveness Directorate, 711th Human Performance Wing, Air Force Research Laboratory, JBSA Fort Sam Houston, TX;
[2]General Dynamics Information Technology, JBSA Fort Sam Houston, TX 78234;
[3]Bioeffects Division, Human Effectiveness Directorate, 711th Human Performance Wing, Air Force Research Laboratory, WPAFB, Dayton, OH
[4]Department of Mechanical and Energy Engineering, University of North Texas, Denton, TX

ABSTRACT

Rapid development in nanomaterial synthesis and functionalization has led to advanced studies in actuation and manipulation of cellular functions for biomedical applications. Often these actuation techniques employ externally applied magnetic fields to manipulate magnetic nanomaterials inside cell bodies in order to drive or trigger desired effects. While cellular interactions with low-frequency magnetic fields and nanoparticles have been extensively studied, the fundamental mechanisms behind these interactions remain poorly understood. Additionally, modern investigations on these concurrent exposure conditions have been limited in scope, and difficult to reproduce. This study presents an easily reproducible method of investigating the biological impact of concurrent magnetic field and nanoparticle exposure conditions using an in-vitro CHO-K1 cell line model, with the purpose of establishing grounds for in-depth fundamental studies of the mechanisms driving cellular-level interactions. Cells were cultured under various nanoparticle and magnetic field exposure conditions from 0 to 500 μg/ml nanoparticle concentrations, and DC, 50 Hz, or 100 Hz magnetic fields with 2.0 mT flux density. Cells were then observed by confocal fluorescence microscopy, and subject to biological assays to determine the effects of concurrent extreme-low frequency magnetic field and nanoparticle exposures on cell-nanoparticle interactions, such as particle uptake and cell viability by MTT assay. Current results indicate little to no variation in effect on cell cultures based on magnetic field parameters alone; however, it is clear that deleterious synergistic effects of concurrent exposure conditions exist based on a significant decrease in cell viability when exposed to high concentrations of nanoparticles and concurrent magnetic field.

Keywords: Magnetic fields, magnetic nanoparticles, nano-manipulation, superparamagnetic, CHO-K1

1. INTRODUCTION

Since the 1970's a multitude of studies have been presented on the effects of magnetic field exposures on various cell lines, particularly at standard distribution frequencies of 50Hz and 60Hz[1–6] and DC magnetic fields[7–9]; many of these studies showing contradictory or irreproducible findings. Because of this, there has been much debate about the effects that external magnetic fields have on cells, and more importantly, it has become clear that the underlying mechanisms driving these effects are still unknown. Additionally, more contradictory results and complications arise when considering cells exposed to both magnetic fields and nanoparticles concurrently[1,7,8,10–14], as studies for the combined effects of these exposures, especially at very low magnetic field frequencies are not yet well established; there are no consistent and agreeable results from these studies showing specific effects derived from concurrent exposures, and most manipulation investigations neglect to focus on extraneous effects.

Previous research has demonstrated that nanoparticle size, shape, surface chemistry, chemical composition, exposure methods and conditions, and even nanoparticle synthesis methods can influence the impact or effects that the particles have on biological systems. It has also been unveiled that any magnetic field-induced cellular effects may depend on a multitude of conditions ranging from cell line, stage in cell cycle, cell age, or even the age of the cells' respective donors.[15-17] Magnetic field-induced cellular level effects may also be very small and difficult to quantify and very minute variations in magnetic field parameters such as field intensity, direction, duration of exposure, and field frequency may have significant impacts on cell behavior, or none at all.[18,19] Despite all of these complications and the decades of debate, magnetic nanoparticle-mediated manipulation of cells and cell structures has been a rapidly growing topic for

Optical Interactions with Tissue and Cells XXVII, edited by E. Duco Jansen
Proc. of SPIE Vol. 9706, 97061Y · © 2016 SPIE · CCC code: 1605-7422/16/$18 · doi: 10.1117/12.2220816

investigation in recent years, with impressive results showing potential toward precise control of cellular behavior and effects. Recent developments in this manipulation-focused research have focused on controlling cellular functions and behavior by shear stress applied by magnetic force-actuation on membrane or surface-bound nanoparticles to activate ion channels and action potentials. More fundamental studies have focused on increasing cell survivability and stress reduction, gene regulation, cell migration, and targeted cell death. These research efforts show the immense potential of cellular nanomanipulation techniques, and also highlight the importance of developing a more complete understanding of the underlying mechanisms behind the magnetic field and nanoparticle interactions on the cellular level.

This paper describes magnetic field, nanoparticle, and combined or concurrent exposure experiments performed on CHO-K1 cell line model to establish grounds for further in-depth mechanistic, proteomic, and genomic studies under standardized conditions. For the purpose of developing future studies, and for independent verification, the magnetic field exposure was conducted using commercially available components, while nanoparticle exposure procedures emulate that of well-established, previously performed toxicological studies.[20] Magnetic field dosimetry was determined first by finite element modeling simulation, and then was measured using a high precision gaussmeter, to ensure consistent magnetic field exposures, and uniform magnetic flux density. Cytotoxicity of the exposures, or respective cell viability and proliferation were measured by trypan blue exclusion method and colorimetric MTT assay. Additionally, mEmerald-tubulin expressing CHO-K1 cells, and Rhodamine-B labeled nanoparticles were used to investigate any physiological impacts or changes in nanoparticle uptake induced by the exposure conditions. For the purpose of simplicity in this paper, the terms “magnetic field” and “magnetic field intensity” refer specifically to the magnitude of magnetic flux density of the induced magnetic fields. These endpoints were chosen based on their relevance to standardized methods of investigation, and the purpose of reproducibility. We believe that establishing a standardized method for investigation of magnetic field effects, and concurrent magnetic field and nanoparticle or other exposures can lead toward the development of more fundamental understandings of underlying mechanisms driving these effects.

2. MATERIALS AND METHODS

2.1 CHO-K1 Cell Culture

The CHO-K1 (ATCC® CCL-61™ Chinese hamster ovary, American Type Culture Collection [ATCC], Manassas, VA) cell line was maintained in Kaighn's modification of Ham's F-12 medium (F-12K Medium) supplemented with 10% volume fetal bovine serum (FBS) (ATCC® 30-2020™) and 1% volume penicillin/streptomycin antibiotics (ATCC® 30-2300). Subculture procedure followed the guidelines set forth by the manufacturer, modified slightly; cells were rinsed with Hank’s Balanced Salt Solution (HBSS, Invitrogen-GIBCO, Waltham, MA), and the subculture ratio used was 1:10, rather than the recommended 1:4, or 1:8 due to the very rapid proliferation rate of the CHO-K1 cells. After the HBSS rinse, the adherent CHO cells were released from the surface of the culture flask by incubation for 5 minutes with 1mL trypsin (Trypsin-EDTA Solution, 1X (ATCC® 30-2101™), followed by dilution in 9mL full serum media. Cells were incubated at 37 °C, 5% CO2 in a Heracell™150i CO2 incubator (Thermo Fisher Scientific Inc., Waltham, MA), in 75 cm2 cell culture flasks and 96-well plates for continued culture, and for exposure conditions respectively. The pH level of the culture media was controlled by 5% CO2 in the incubation chamber, in combination with sodium bicarbonate concentration (1,500mg/mL) in media. For visualization of microtubule cytoskeleton, CHO cells were transfected with a mEmerald-tubulin plasmid (a kind gift from Mr. Michael W. Davidson of the National High Magnetic Field Laboratory at Florida State University, Tallahassee, FL) using Effectene (#301425; Qiagen, Gaithersburg, MD) and maintained with G418 sulfate solution (#345812, Calbiochem, Philadelphia, PA). The stable transfection of the CHO cell line was performed by Dr. Marjorie Kuipers and provided as a generous gift from the U.S. Air Force Research Laboratories (Fort Sam Houston, TX).

2.2 Magnetic Field Exposure and Dosimetry

For magnetic field exposure conditions, cells were cultured in the 96-well plates, and were placed in the center of a SpinCoil-7-X Helmholtz coil system purchased from MicroMagnetics (Fall River, MA). Driving current was supplied, and easily regulated (from 110V 60Hz line-source) by a variable-voltage, variable-frequency Kikusui PCR500M Compact AC Power Supply (Kikusui Electronics Corporation, Yokohama, Japan), allowing for precise control of the system (0-270VAC, DC, 40-400Hz). A Helmholtz coil was selected as the desired magnetic field generation configuration due to the mostly-uniform magnetic field generated over a reasonably large area at the center of the coils.[21–23] The Helmholtz coil was placed inside a NuAire Autoflow CO2 Water-Jacketed Incubator (NuAire Plymouth, MN), maintained at 37 °C, 5% CO2, and power-supply run through an insulated port in the side of the chamber. The

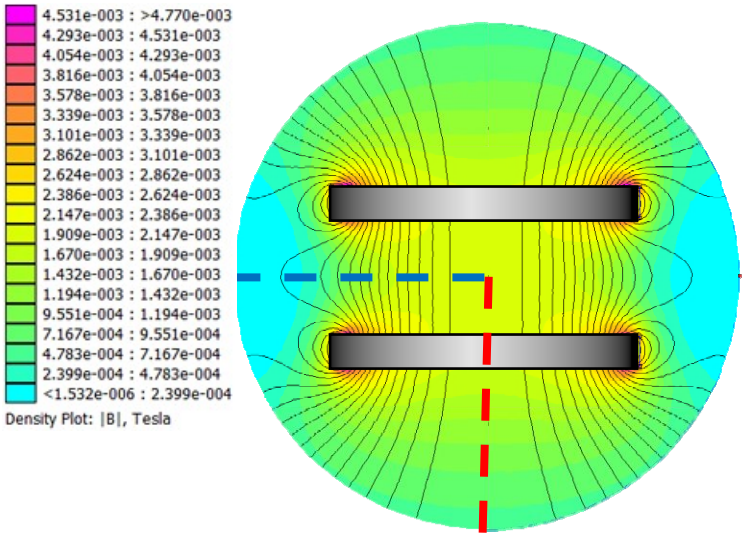

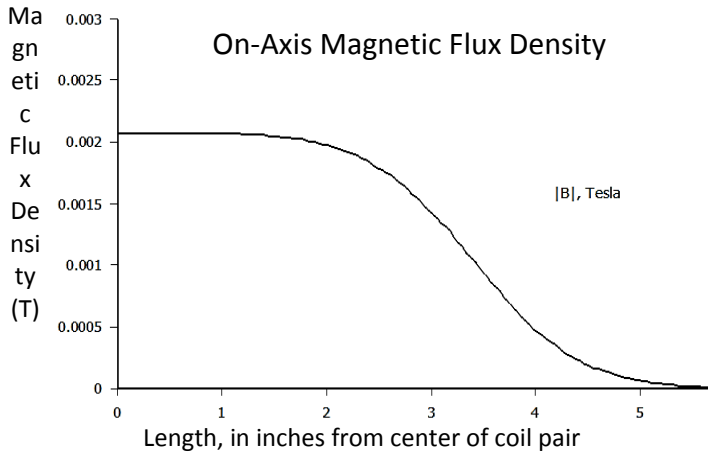

Figures 1-2: FEMM simulation: Flux density plot for cross section cut of magnetic field produced by Helmholtz coil pair. Below is shown a flux density measurement from Helmholtz coil center, along either X or Y axis as depicted above.

magnetic flux density was measured at multiple points across the area through which cell culture plates were exposed, using a Lakeshore 425 Gaussmeter and LakeShore Fiberglass Transverse Probe HMNT-4E04-VR (LakeShore Cryotronics Inc Westerville, OH). The Helmholtz coil was powered for one hour before cell culture-exposure began, allowing any heating and resistive change in the circuit to occur prior to executing the experiment. There was no measurable temperature rise within the exposure chamber, or region near cell culture during operation of the Helmholtz coil system, however there was a minor change in current measured through the coil before stabilizing after 15-20 minutes of operation. The power to the coil was briefly cut off when inserting and removing each cell culture dish, to prevent any unintended magnetic field effects on the particles as they moved into, and through the field, as a closed circuit would continue to produce a magnetic field, and thus a Lorentz force would be exerted on the particles as they moved through the field. In all experiments reported, field intensity was measured at 2.0mT (rms), uniform to within ± 4% over the cell exposure area, with DC, 50Hz, and 100Hz driving current for each respective experiment. Finite Element Method Magnetics (FEMM 4.2) software was used to simulate the magnetic field and flux density generated by the Helmholtz coil given the specific driving currents (Figure 1 and 2). The specific magnetic field parameters of 2.0mT, DC and 50Hz fields were selected because they have been frequently investigated for impact on cellular behavior[2–5,7,9,24,25], and because 50Hz and 60Hz are common frequencies at which electric power distribution lines operate worldwide.[26] Additionally, a DC field was selected to provide insight about field interactions with the cells and particles, as compared to alternating frequency effects. 100Hz frequency was selected to determine any specific frequency dependent or frequency specific effects between 0Hz (DC), 50Hz, and 100Hz exposures. In addition, the 100Hz frequency experiment was selected in order to gleam insight towards the magnetic field-nanoparticle interactions, and to investigate if a higher extreme-low frequency magnetic field would have an increased effect on nanoparticle uptake, and cell viability. For all exposure conditions, a respective parallel sham experiment was performed and used as a control group. Shams were placed in the same incubation chamber as the magnetic field-exposed cells, at a distance such that the magnetic field generated by the Helmholtz coil was negligible. This was possible due to the $1/r^2$ relation of magnetic field strength, where r is the distance from a magnetic field source; the magnetic field strength falls off very rapidly away from the source of the field, and therefore only a short distance outside of the coil system, the magnetic field strength is negligible. This procedure worked to ensure that any potential variability between additional environmental strain between the exposed group, and the control group was related specifically to the magnetic field exposure, and not additional conditions related to being in separate incubation chambers.

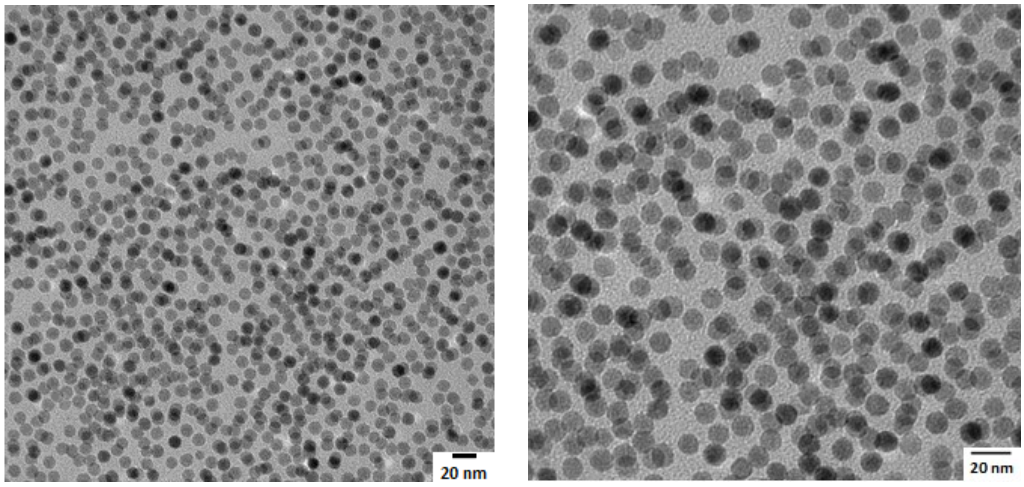

Figure 3: TEM imaging of Fe_3O_4 nanoparticles performed to verify spherical shape and particle

2.3 Nanoparticles and Characterization

Two sets of commercially available iron oxide particles were purchased, 10nm Fe3O4 particles dispersed in double-distilled water at a concentration of 5mg/mL from Cytodiagnostics (Burlington, Ontario, CA), and Rhodamine-B labeled 10nm Fe2O3 particles dispersed in DI water at a concentration of 1 mg/mL (Fe) from Ocean NanoTech (Springdale, AR). The non-labeled particles were characterized through transmission electron microscopy (TEM; Figure 3) dynamic light scattering (DLS) polydispersity index (PdI) and zeta potential. Dynamic light scattering is a non-destructive method for measuring size and size distribution of particles in a colloidal solution. Zeta potential measurements can be used as an indicator of electrostatic repulsion between the particles in a colloidal solution; the greater in magnitude the zeta potential measurement, the more stable the particles in the colloidal solution should be. The PdI is a measure of particle and agglomerate s ize distribution. Low PdI values indicate a very small size distribution, while larger numbers indicate a very large size distribution. Very large values, from 0.7-1 indicate that DLS may not provide very accurate measurements of particle size or hydrodynamic diameter, due to the large size distribution of particle agglomerates. DLS, Zeta Potential, and PdI measurements were all taken using a Zetasizer Nano (Malvern Instruments Ltd, Malvern, Worcestershire, UK), system at the University of Texas, San Antonio (with gracious assistance from Ms. Samantha Franklin). TEM imaging was performed with a 120kV PC Hitachi H-7600 controlled TEM (Hitachi Ltd. Chiyoda, Tokyo, Japan) and was provided courtesy of Elizabeth Maurer-Gardner (Research Scientist, Materials Characterization Specialist AFRL, Dayton, OH). Particle size was observed to be 10.97 ± 0.70 nm, based on the measurement of 50 independent nanoparticles. DLS and zeta potential characterization was performed for samples of nanoparticle-water, and nanoparticle-media dilutions at concentrations of 50, and 200 μg/mL in water, and 50, 200, and 500 μg/mL in media, under conditions with and without 24 hour DC magnetic field exposure. These dilutions were chosen to get an understanding of how the concentration of the particle dilution impacts agglomerate behavior under various conditions. Based on other scientific reports, it was expected that the particles would agglomerate, due to protein-particle interaction in cell media, and the particles' induced magnetization when subject to the application of a large external magnetic field[12,27–29]; therefore DC magnetic field exposure was selected to induce the greatest possible magnetization of the particles, and because preliminary results led us to believe that DC fields had the greatest impact on cell viability under concurrent exposure conditions. The zeta potential of the particles dispersed in water was that of a moderately stable colloidal solution, with magnitude ranging from 16.2 to 38.2 mV, however the PdI was very high for the lowest concentration of particles both with and without magnetic field exposure, at 0.94-0.96, indicating that the particles had begun to sediment and settle in the solution. The average hydrodynamic diameter was measured at 1248nm and 518.2nm for the 50 μg/mL concentration in water with and without magnetic field exposure respectively, indicating that the average agglomerate size is larger with magnetic field exposure, even with sedimentation. At the higher concentration of 200μg/mL the colloidal solution appeared to be more stable, with PdI around 0.33-0.35, and average hydrodynamic diameter measurements in the expected range of approximately 20nm and 50nm with and without magnetic field exposure respectively. For particles dispersed in media, the zeta potential was measured significantly closer to zero, or near-neutral, with magnitude ranging from 0.16 to 9.0 mV. A near-neutral zeta potential indicates that the particles may agglomerate or coagulate fairly rapidly, however the PdI measured for all but one sample, was measured below 0.7,

indicating reliable size measurements, or small size distribution of particle agglomerates. Of most importance to this study, are the magnitudes of zeta potential measurements from particle-media dilution samples, which are all less than 10, with hydrodynamic diameters ranging from 50nm – 1 μm when exposed to magnetic field. The Rhodamine-B labeled particles were used for fluorescence microscopy experiments only, and therefore were not a focus of characterization study. The manufacturer report indicates that the Rhodamine-B labeled particles have a near-neutral zeta potential, and particle size of 10nm ± 2.5nm, with size distribution of ~10%. Ultimately, this difference between the Rhodamine-B labeled particles and the non-labeled particles is not of great concern in this particular study, as all statistically significant effects were observed at very high Fe3O4 concentrations, where the respective measurements in media closely reflect this same behavior**.**

2.4 MTT Assay – Cell Viability and Mitochondrial Function

To assess cell mitochondrial function, and thereby viability or proliferation, a colorimetric MTT (3-(4, 5-dimethylthiazolyl-2)-2, 5-diphenyltetrazolium bromide) assay was used (ATCC ® 30-1010K™). [30] Using the aforementioned culture methods, cells were plated at 2 x 10^5 cells/mL into 96 well plates at 50μl/well, giving approximately 1 x 10^4 cells per well, and then exposed to each respective exposure condition six hours later. After 24 hours of continuous exposure, the cell media and nanoparticles were aseptically removed, and the wells were refilled with a mixture of 100μl full cell media, and 10μl MTT tetrazolium salt reagent. The cells were let sit for two hours, before 100μl of detergent was added to each well to dissolve formazan crystals. The plates were then wrapped in aluminum foil, and placed on a benchtop orbital shaker at room temperature, overnight; absorbance readings were taken the following morning. Background readings were taken from wells that were treated identical to the experiment wells, with the exception that there were no cells plated. These background cells allowed for analysis to consider any residual particles that may have been left in the wells and their potential interference with the absorption readings from the microplate reader. An effective dose (ED50) was calculated to determine the concentration of the particles that successfully reduced the cell population to a fraction of half the control value, after the exposure time is complete.

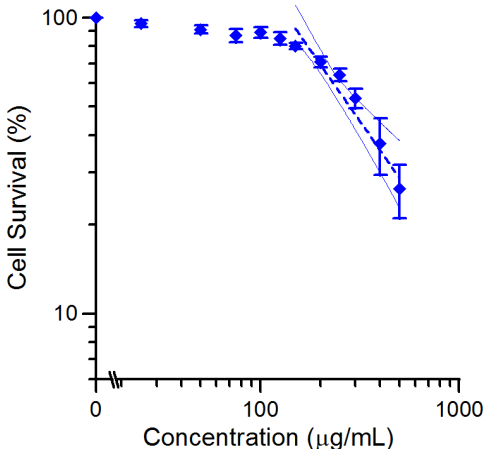

Figure 4: MTT Concentration-dependent survivability curve of cells exposed to Fe_3O_4 nanoparticles and no magnetic field with 95% confidence interval.

2.5 Confocal Microscopy and Particle Uptake

To observe cell morphology, microtubule formation, and nanoparticle uptake with and without magnetic field exposure, the Rhodamine-B labeled nanoparticles were added to cells cultured in poly-D-lysine coated glass-bottom dishes six hours after the cells were plated. Immediately following the addition of the nanoparticle solution, the culture dishes were placed in respective exposure and sham positions in the exposure incubation chamber for 24 hours. A Zeiss LSM 710 confocal microscope (Carl Zeiss MicroImaging GmbH, Jena, Germany) with DIC40X 1.2NA objective (Carl Zeiss MicroImaging) was used in conjunction with the ZEN 2012 software (Zen 2012 SP1 Black Edition – Ver. 8,1,3,484, Carl Zeiss Microscopy GmbH) to image the mEmerald-tubulin expressing CHO-K1 cells and Rhodamine-B labeled nanoparticles. The peak excitation and emission wavelengths for mEmerald and Rhodamine-B are 487/509 and 540/625 respectively, and the pinhole was adjusted for 1μm sections for all time-series imaging. For various positions on the culture dishes, multiple images were taken in time series - 30 cycles at a rate of one cycle every 12 seconds, for a total period of six minutes, to observe cell-nanoparticle interaction, intracellular trafficking, and tubulin change. Single image acquisition of CHO cells with fluorescent tubulin expression was done with a line step of one, and line average four to acquire clear images of microtubule formations. Numerical values were obtained by mean fluorescence of cells exposed to Rhodamine-B labeled nanoparticles, which was measured and compared between cells subjected to DC magnetic field exposure and those of sham exposure conditions. As microtubules have been identified as playing a significant role in vesicular intracellular trafficking[31], CHO-K1 cells with both mEmerald-tubulin expression and nanoparticle exposures were imaged after magnetic field and sham exposure conditions, in an attempt to observe any changes in tubulin-nanoparticle interaction, tubulin expression, and microtubule structure and formation. The public domain Java-based program Fiji[32] was used for independent image and image-series processing.

3. RESULTS

The cytotoxicity of 10nm Fe3O4 nanoparticles was assessed by means of MTT assay, for magnetic field exposures at DC, 50Hz, and 100Hz frequencies. The measurements for nanoparticle exposure without any applied external magnetic field are displayed in figure 4, and as sham exposures in Figure 5a-c. These results closely resemble those of other reported toxicity assessments for Fe3O4 particles[20,33,34], showing a minor increase in mitochondrial activity at very low doses ~10µg/mL, and significant reduction at extremely high concentrations, upward of 250µg/mL and higher. Additional assays were performed for cells cultured under nanoparticle and concurrent (DC, 50Hz, or 100Hz) magnetic field, or respective sham exposure conditions. The ED50 value for nanoparticle (no magnetic field) exposure was calculated at 370µg/mL, which is also in agreement with previous studies. Statistical significance compared to controls was determined using Student's unpaired t-test with two-tailed P value < 0.05. MTT assay results for the various magnetic field exposure conditions showed a minor increase in viability at low Fe3O4 nanoparticle concentration in most trials; however the difference was not statistically significant when compared to sham conditions. At higher nanoparticle concentration, there was observed a marked reduction in cell viability, when compared to the respective sham exposures. Our data suggests a trend of reduced cytotoxicity with increased magnetic field frequency; the DC magnetic field appears to have the most significant reduction on cell viability, followed by 50Hz, and finally, the least significant impact on cell viability has been observed with the 100Hz magnetic field exposure. A compilation for comparison of all exposure conditions is displayed in Figure 5.

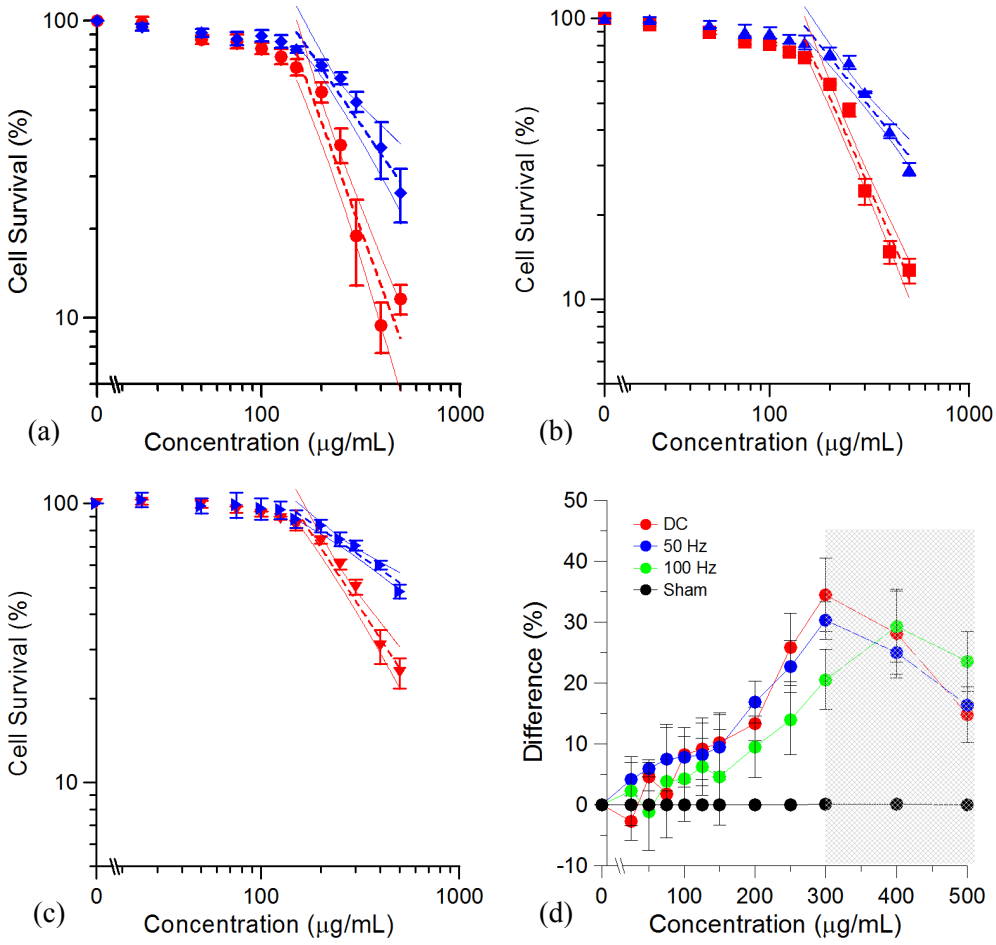

Figure 5: MTT Concentration-dependent survivability curves for cells exposed (red) vs sham (blue) for Fe_3O_4 nanoparticles and (a) DC magnetic field, (b) 50Hz magnetic field (c) 100Hz magnetic field, and (d) the respective Δ from sham conditions. The greyed section represents the area beyond the ED_{50} for cells not exposed to magnetic fields. Sham exposure Δ measured against trials in an independent incubator. Interval fits represent 95% confidence.

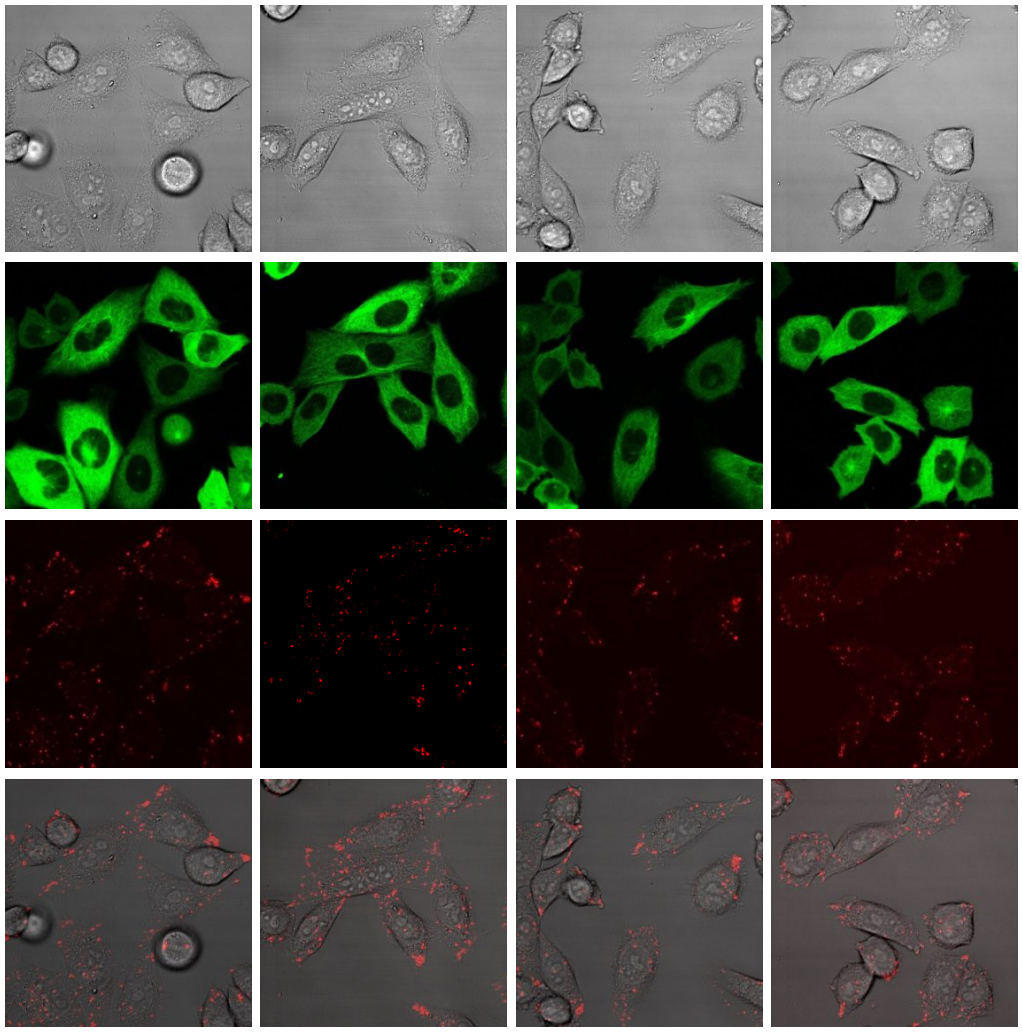

Figure 6: Select images from confocal microscopy study without DC magnetic field exposure; (a) bright field images (b) Fluorescent mEmerald tubulin expression (c) Fluorescence imaging with Rhodamine-B labeled particles and (d) Overlay results from bright field and Rhodamine-B fluorescence imaging to show particles inside the cell structures.

For particle uptake, cytoskeletal structure and tubulin network analysis, confocal fluorescent microscopy image analysis showed that the mEmerald-tubulin expressing cells (Figure 6b) demonstrated no significant difference in tubulin network after magnetic field, or concurrent magnetic field and nanoparticle exposures; however there was measured a significant impact on particle uptake and localization due to magnetic field exposures, especially with nanoparticle exposures of very lower concentrations (figure 7). The Rhodamine-B labeled Fe_2O_3 particles were observed to be endocytosed, or taken into the cells, and trafficked throughout the cells (figure 6c-d). Little to no nanoparticles were observed within the perinuclear region of the cells, but clusters were observed in what are likely lysosomal structures within the cells.

4. DISCUSSION

Though the MTT assay appears to show a correlation between magnetic field frequency and cell viability or mitochondrial activity, it may be beneficial to reproduce the experiments for increased accuracy, as all three magnetic field exposures do appear to have the same general effect on the cells; the apparent decrease in toxicity with 100Hz magnetic field exposure, compared to DC and 50Hz frequency conditions may be the result of a small variation in

dilution for those exposure conditions introduced by pipette and dilution error. This may be concluded by data shown in Figure 5d, a graph showing the respective difference in survival from exposure and sham conditions. The 100Hz delta curve follows almost exactly the curves of the DC and 50Hz exposures, with a right-shift of one concentration value, and peaks with the same trend. The ED50 of each exposure condition was calculated by interpolation as 370μg/mL, 217μg/mL, 237.4μg/mL, and 303.3μg/mL for no magnetic field, DC, 50Hz, and 100Hz, respectively. The differences between ED50 for each magnetic field exposure may yet again be attributed to the right-shift in delta mentioned previously. This suggests that there may be no difference in the effect of 2.0mT DC, 50Hz, and 100Hz frequency magnetic fields exposures on the CHO-K1 cell line. This information is contradictory to the argument that the frequency of externally applied magnetic fields would have a direct effect on the response or behavior of the cells, and suggests that at extremely-low frequencies, the effects of magnetic fields and concurrent magnetic field-nanoparticle exposures are frequency independent.

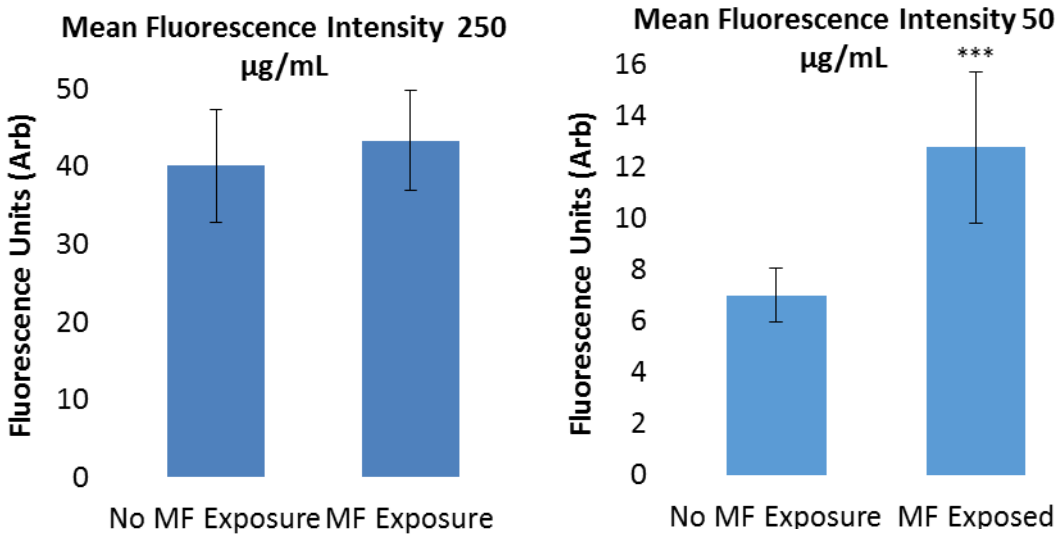

Figure 7: Mean fluorescence intensity of cells measured with, and without DC magnetic field exposure at nanoparticle concentrations of 250 μg/mL and 50 μg/mL respectively. The impact of magnetic field exposure on particle uptake is much more significant at the lower particle concentrations.

Due to the prominence of the DC field on cytotoxicity and cell viability measurements in the initial studies, all fluorescence and microscopy studies were performed with DC magnetic field exposure conditions in an attempt to investigate the cellular physiology effects of the exposures though we report no measurable difference in tubulin network density, higher resolution imaging, or an improved analysis algorithm may be useful in reproducing the experiment. Additional labeling methods for tracking lysosomal structures, such as LysoTracker Red can also be used to confirm the nanoparticle locations in lysosomes, and for real-time imaging of nanoparticle and cell behavior when directly under magnetic field exposure conditions; this should help to further elucidate the mechanisms behind the decreased cell viability from concurrent exposure conditions. Future experiments will include variable frequency exposures, increased line averaging, higher resolution imaging, and more rapid image capture, to enhance image clarity and analysis, as well as further investigations of mitochondrial response to magnetic field and nanoparticle exposures by method of oxidative consumption rate (OCR) and recovery from modulation and induced inhibition

ACKNOWLEDGEMENTS

The authors would like to thank Dr. Gary Thompson (Oak Ridge Institute for Science and Education, JBSA Fort Sam Houston, Texas) and Mr. Caleb Roth (University of Texas Health Science Center at San Antonio, Department of

Radiological Sciences, San Antonio, Texas) for assistance with cell culture techniques and confocal microscopy image acquisition, processing, and analysis, as well Mrs. Samantha Franklin (University of Texas at San Antonio, Department of Physics, San Antonio, Texas) for assistance with DLS, ZetaPotential and PdI measurements of the Fe_3O_4 nanoparticles, and Mrs. Elizabeth Maurer-Gardner (Research Scientist, Materials Characterization Specialist AFRL, Dayton, OH) for TEM imaging of Fe_3O_4 particles. This study was supported by seedling funds from the 711th Human Performance Wing Chief Scientists Office.

REFERENCES

[1] Zhang, Y., Ding, J.., Duan, W., "A study of the effects of flux density and frequency of pulsed electromagnetic field on neurite outgrowth in PC12 cells," Journal of biological physics **32**(1), 1–9, Springer (2006).

[2] Pozzi, D., Grimaldi, S., Ledda, M., De Carlo, F., Modesti, A., Scarpa, S., Foletti, A.., Lisi, A., "Effect of 50 Hz Magnetic Field exposure on Neuroblastoma Morphology," IJIB **1**, 12–16 (2007).

[3] Hasanzadeh, H., Rezaie-Tavirani, M., Seyyedi, S. S., Zali, H., Keshel, S. H., Jadidi, M.., Abedelahi, A., "Effect of ELF-EMF Exposure on Human Neuroblastoma Cell Line: a Proteomics Analysis," Iranian journal of cancer prevention **7**(1), 22, Shahid Beheshti University of Medical Sciences (2014).

[4] Falone, S., Sulpizio, M., Angelucci, S., Marchisio, M., Di Giuseppe, F., Eleuterio, E., Di Ilio, C.., Amicarelli, F., "Extremely low frequency magnetic field-induced effects on cell biology and proteome expression of a human neuroblastoma cell line."

[5] Cerrato, C., Cialdai, F.., Monici, M., "Effects of Low Frequency Electromagnetic Fields on SHSY5Y cells-a neuroblast model," Energy for Health **8**, 18–24 (2011).

[6] McFarlane, E. H., Dawe, G. S., Marks, M.., Campbell, I. C., "Changes in neurite outgrowth but not in cell division induced by low EMF exposure: influence of field strength and culture conditions on responses in rat PC12 pheochromocytoma cells," Bioelectrochemistry **52**(1), 23–28, Elsevier (2000).

[7] Prijic, S., Scancar, J., Cemazar, M., Bregar, V. B., Znidarsic, A., Sersa, G.., others., "Increased cellular uptake of biocompatible superparamagnetic iron oxide nanoparticles into malignant cells by an external magnetic field," The Journal of membrane biology **236**(1), 167–179, Springer (2010).

[8] Comfort, K. K., Maurer, E. I.., Hussain, S. M., "The biological impact of concurrent exposure to metallic nanoparticles and a static magnetic field," Bioelectromagnetics **34**(7), 500–511, Wiley Online Library (2013).

[9] Ahmadianpour, M. R., Abdolmaleki, P., Mowla, S. J.., Hosseinkhani, S., "Static magnetic field of 6 mT induces apoptosis and alters cell cycle in p53 mutant Jurkat cells," Electromagnetic biology and medicine **32**(1), 9–19, Informa Healthcare New York (2013).

[10] Hughes, S., McBain, S., Dobson, J.., El Haj, A. J., "Selective activation of mechanosensitive ion channels using magnetic particles," Journal of The Royal Society Interface **5**(25), 855–863, The Royal Society (2008).

[11] Tseng, P., Judy, J. W.., Di Carlo, D., "Magnetic nanoparticle-mediated massively parallel mechanical modulation of single-cell behavior," Nature methods **9**(11), 1113–1119, Nature Publishing Group (2012).

[12] Skebo, J. E., Grabinski, C. M., Schrand, A. M., Schlager, J. J.., Hussain, S. M., "Assessment of metal nanoparticle agglomeration, uptake, and interaction using high-illuminating system," International journal of toxicology **26**(2), 135–141, SAGE Publications (2007).

[13] Fanelli, C., Coppola, S., Barone, R., Colussi, C., Gualandi, G., Volpe, P.., Ghibelli, L., "Magnetic fields increase cell survival by inhibiting apoptosis via modulation of Ca2+ influx," The FASEB Journal **13**(1), 95–102, FASEB (1999).

[14] Zhang, E., Kircher, M. F., Koch, M., Eliasson, L., Goldberg, S. N.., Renström, E., "Dynamic magnetic fields remote-control apoptosis via nanoparticle rotation," ACS nano **8**(4), 3192–3201, ACS Publications (2014).

[15] Simkó, M., Kriehuber, R., Weiss, D. G.., Luben, R. A., "Effects of 50 Hz EMF exposure on micronucleus formation and apoptosis in transformed and nontransformed human cell lines.," Bioelectromagnetics **19**(2), 85–91 (1998).

[16] Cadossi, R., Bersani, F., Cossarizza, A., Zucchini, P., Emilia, G., Torelli, G.., Franceschi, C., "Lymphocytes and low-frequency electromagnetic fields.," The FASEB journal **6**(9), 2667–2674, FASEB (1992).

[17] Walleczek, J.., Budinger, T. F., "Pulsed magnetic field effects on calcium signaling in lymphocytes: dependence on cell status and field intensity.," FEBS Lett. **314**(3), 351–355 (1992).

[18] Goodman, R.., Henderson, A. S., "Exposure of salivary gland cells to low-frequency electromagnetic fields alters polypeptide synthesis," Proceedings of the National Academy of Sciences **85**(11), 3928–3932, National Acad Sciences (1988).
[19] Balcer-Kubiczek, E. K., Harrison, G. H., Davis, C. C., Haas, M. L.., Koffman, B. H., "Expression analysis of human HL60 cells exposed to 60 Hz square- or sine-wave magnetic fields.," Radiat. Res. **153**(5 Pt 2), 670–678 (2000).
[20] Hussain, S., Hess, K., Gearhart, J., Geiss, K.., Schlager, J., "In vitro toxicity of nanoparticles in BRL 3A rat liver cells," Toxicology in vitro **19**(7), 975–983, Elsevier (2005).
[21] Cvetkovic, D.., Cosic, I., "Modelling and design of extremely low frequency uniform magnetic field exposure apparatus for in vivo bioelectromagnetic studies," Engineering in Medicine and Biology Society, 2007. EMBS 2007. 29th Annual International Conference of the IEEE, 1675–1678 (2007).
[22] DeTroye, D. J.., Chase, R. J., "The Calculation and Measurement of Helmholtz Coil Fields" (1994).
[23] Bhatt, V., Rautela, R., Sharma, P., Tiwari, D.., Khushu, S., "Design & Development of Helmholtz Coil for Hyperpolarized MRI."
[24] Gamboa, O., Gutiérrez, P., Alcalde, I., De la Fuente, I.., Gayoso, M., "Absence of relevant effects of 5 mT static magnetic field on morphology, orientation and growth of a rat Schwann cell line in culture," Murcia: F. Hernández (2007).
[25] Ghodbane, S., Lahbib, A., Sakly, M.., Abdelmelek, H., "Bioeffects of static magnetic fields: oxidative stress, genotoxic effects, and cancer studies," BioMed research international **2013**, Hindawi Publishing Corporation (2013).
[26] Portier, C. J.., Wolfe, M. S., "Assessment of health effects from exposure to power-line frequency electric and magnetic fields," NIH publication **98**, 3981 (1998).
[27] Tschulik, K.., Compton, R. G., "Nanoparticle impacts reveal magnetic field induced agglomeration and reduced dissolution rates," Physical Chemistry Chemical Physics **16**(27), 13909–13913, Royal Society of Chemistry (2014).
[28] Lim, E. W. C.., Feng, R., "Agglomeration of magnetic nanoparticles," The Journal of chemical physics **136**(12), 124109, AIP Publishing (2012).
[29] Papaefthymiou, G. C., "Nanoparticle magnetism," Nano Today **4**(5), 438–447, Elsevier (2009).
[30] Mosmann, T., "Rapid colorimetric assay for cellular growth and survival: application to proliferation and cytotoxicity assays," Journal of immunological methods **65**(1), 55–63, Elsevier (1983).
[31] Matteoni, R.., Kreis, T. E., "Translocation and clustering of endosomes and lysosomes depends on microtubules.," The Journal of cell biology **105**(3), 1253–1265, Rockefeller Univ Press (1987).
[32] Schindelin, J., Arganda-Carreras, I., Frise, E., Kaynig, V., Longair, M., Pietzsch, T., Preibisch, S., Rueden, C., Saalfeld, S., et al., "Fiji: an open-source platform for biological-image analysis," Nature methods **9**(7), 676–682, Nature Publishing Group (2012).
[33] Mahmoudi, M., Simchi, A., Milani, A.., Stroeve, P., "Cell toxicity of superparamagnetic iron oxide nanoparticles," Journal of colloid and interface science **336**(2), 510–518, Elsevier (2009).
[34] Bae, J.-E., Huh, M.-I., Ryu, B.-K., Do, J.-Y., Jin, S.-U., Moon, M.-J., Jung, J.-C., Chang, Y., Kim, E., et al., "The effect of static magnetic fields on the aggregation and cytotoxicity of magnetic nanoparticles," Biomaterials **32**(35), 9401–9414, Elsevier (2011).